Available online at www.sciencedirect.com
SCIENCE DIRECT®
Journal of Power Sources 135 (2004) 344–353
JOURNAL OF POWER SOURCES
www.elsevier.com/locate/jpowsour

Effect of heat treatment on material characteristics and pseudo-capacitive properties of manganese oxide prepared by anodic deposition

Jeng-Kuei Chang, Yi-Lun Chen, Wen-Ta Tsai*

Department of Materials Science and Engineering, National Cheng Kung University, Tainan 70101, Taiwan

Received 22 January 2004; accepted 30 March 2004

Available online 26 June 2004

Abstract

Hydrous manganese oxide with amorphous structure is prepared by anodic deposition in manganese acetate solution. The effect of heat treatment (100–700 °C) on the material characteristics of the oxides is investigated. The thermal property of the deposited oxide is examined by thermogravimetric and differential thermal analyses. Dehydration, organic-matter decomposition, oxidation and crystallization of the manganese oxide as a function of temperature are examined. Glancing angle X-ray diffraction, scanning electron microscope and X-ray photoelectron spectroscopy are carried out to explore, respectively, the crystal structure, surface morphology and chemical state of the oxide electrodes. It is found that the as-deposited manganese oxide, with an amorphous structure and fibrous feature, is further oxidized and tends to tangle with increasing annealing temperature (below 500 °C). When the temperature uses above 500 °C, the formation of crystalline oxide is confirmed. Cyclic voltammetry is also performed to evaluate the electrochemical performance of the oxide electrodes annealed at various temperatures. Excellent pseudo-capacitive behaviour of the oxide electrodes is revealed at a low annealing temperature (≤200 °C). The cyclic stability of the deposited manganese oxide is significantly improved by introducing proper heat treatment.

Keywords: Manganese dioxide; Pseudo-capacitors; Heat treatment; Cyclic voltammetry; Anodic deposition

1. Introduction

Electrochemical pseudo-capacitors are charge-storage devices that have greater power density and longer cycle-life than batteries, and possess higher energy density compared with conventional capacitors [1]. They have recently been considered to be promising devices in many fields, e.g., hybrid power sources, peak-power sources, back-up power storage, lightweight electronic fuses, starting power for fuel cells [2–4]. Pseudo-capacitance arises from a fast, reversible, faradaic redox reaction that occur near an electrode surface over an appropriate range of potentials [2,5–7]. Amorphous hydrous ruthenium oxide prepared by the sol–gel process has been demonstrated to exhibit pseudo-capacitive behaviour and be a potential electrode material for use in supercapacitors [5]. A strong dependence of its specific capacitance on the crystal structure, governed by annealing temperature, has also been reported [6]. The largest specific capacitance (over 700 F g^{-1}), with excellent reversibility, of the oxide was obtained at 150 °C which is just below the crystallization temperature. The high cost of ruthenium has, however, limited its commercial use. Therefore, the search for a cheaper oxide with equivalent characteristics is attracting attention.

The natural abundance of manganese oxide and its environmental compatibility make it the subject of increasing research interest. Recently, several workers have begun to develop effective methods for producing manganese oxide [8–16]. The material characteristics and electrochemical properties of the oxides prepared by various processes, including thermal decomposition [10], co-precipitation [11], sol–gel process [12–14] and anodic deposition [15,16] have been found to be quite different. Interestingly the effects of heat treatment, though very important, have not been extensively studied. Jeong and Manthiram [9] reported that nanocrystalline manganese oxide, with good pseudo-capacitive properties could be synthesized by reducing aqueous $KMnO_4$ solution with various agents, e.g., potassium borohydride. The resulting oxide was heated in the range of 50–150 °C. The crystal structure did not vary with temperature within this range, but a maximum specific capacitance was found at 75 °C. This phenomenon is different from that for ruthenium oxide, as mentioned above

* Corresponding author. Tel.: +886 6275 4395; fax: +886 6275 4395.
E-mail address: wttsai@mail.ncku.edu.tw (W.-T. Tsai).

0378-7753/$ – see front matter © 2004 Elsevier B.V. All rights reserved.
doi:10.1016/j.jpowsour.2004.03.076

[6]. Unfortunately, no further analytic data about the oxide were presented to explain the observed behaviour, Pang and coworkers [12,13] manufactured manganese oxides by a sol–gel process and electrodeposition. The electrochemical and material-property analyses mainly focused on the as-prepared and 300 °C-annealed oxides. The specific capacitance and cyclic stability of both types of oxide were improved after heat treatment at 300 °C. Oxides annealed at other temperatures were not well discussed. Clearly, a thorough and systematic study about the effects of heat treatment on material characteristics and pseudo-capacitive properties of the manganese oxide is indeed worthy of investigation.

In this study, manganese oxides prepared by anodic deposition in manganese acetate solution are heat treated between 100 and 700 °C. The corresponding crystal structure, surface morphology, composition, chemical state and electrochemical performance of the oxides as a function of annealing temperature have been extensively examined.

2. Experimental

Manganese oxide was electroplated on to 1 cm × 1 cm graphite substrates by anodic deposition in a neutral 0.25 M $Mn(CH_3COO)_2$ plating solution at 25 °C. The substrates were first polished with SiC paper of 800 grit, degreased with acetone and water, etched in 0.2 M H_2SO_4 at 25 °C, and finally washed with pure water in an ultrasonic bath. During deposition, the graphite substrate was held as the anode and a platinum sheet was used as the counter electrode. A saturated calomel electrode (SCE) was employed as a reference electrode. An EG&G Princeton Applied Research model 263 potentiostat was employed to control the deposited conditions. Anodic deposition was performed under constant applied potential. The applied potential was 0.5 V (versus SCE) to give a total delivered charge of 1.5 C. After electrodeposition, the electrode was dried in air. The amount of manganese oxide loaded on to the carbon substrate was then weighed using a microbalance with an accuracy of 1×10^{-5} g. A Setaram TGA 92 analyzer was used to perform simultaneous thermogravimetric and differential thermal analyses (TG/DTA). Deposited manganese oxide, detached from the graphite substrate, was heated from 25 to 900 °C at a rate of 10 °C/min under a flowing air atmosphere. The flow rate was 20 mL/min and α-Al_2O_3 was used as the reference material.

The manganese oxide electrodes were annealed at various temperatures (to 700 °C) for 2 h. The crystal structure of the oxide electrodes was determined by glancing angle X-ray diffraction (GAXRD). The patterns were recorded on a Rigaku D/MAX-2500 diffractometer with a glancing incident angle of 1°. Kα_1 radiation of a copper target with a wavelength of 1.54056 Å was used as the X-ray source. The detected diffraction angle (2θ) was scanned from 20 to 80° with a speed of 4°/min. The surface morphologies of the manganese oxides, annealed at various temperatures, were observed by means of a scanning electron microscope (SEM, Philip XL-40FEG). An auxiliary X-ray energy dispersive spectroscope (EDS) was used to examine the chemical composition of the oxides electrodes. X-ray photoelectron spectroscopy (XPS) was also carried out to evaluate the chemical state of the manganese oxides. The measurements were performed with an ESC A 210 (VG Science Ltd.) spectrometer. Monochromated Al Kα (1486.6 eV) radiation served as the X-ray source. The pressure in the analyzing chamber was approximately 1×10^{-9} Torr during the measurements.

The electrochemistry of manganese oxide was characterized by cyclic voltammetry (CV) in 2 M KC1 solution at room temperature. The test cell was a three-electrode system in which the manganese oxide electrode was assembled as the working electrode. A platinum sheet and a saturated calomel electrode were used as the counter electrode and the reference electrode, respectively. The measuring instrument was an EG&G M263 potentiostat. The potential was cycled within a potential range of 0–1 V (versus SCE). The CV scan rate was varied from 5 to 150 mV s^{-1}.

3. Results and discussion

3.1. TG and DT analyses of deposited manganese oxide

A TG/DTA plot of the as-deposited manganese oxide, detached from the substrate, is shown in Fig. 1 for a heating rate of 10 °C/min in air atmosphere. The weight and enthalpic changes as a function of temperature are demonstrated in this figure. The initially sharp weight loss, corresponding to an endothermic reaction, occurs below 100 °C.

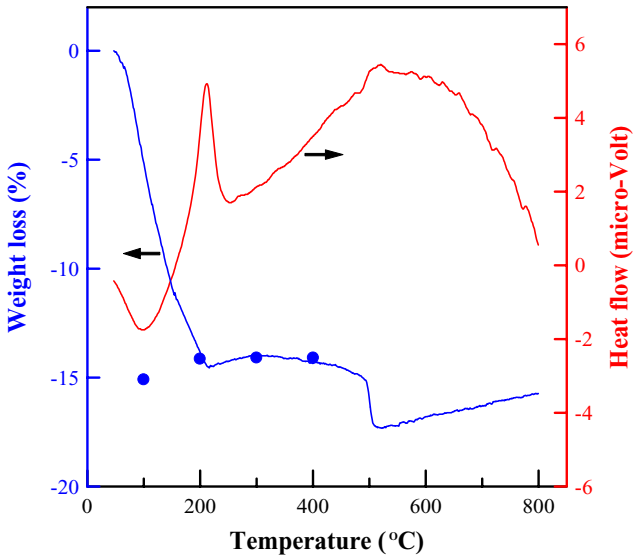

Fig. 1. TG/DTA plot of as-deposited manganese oxide at heating rate of 10 °C/min in air atmosphere; (●) denotes weight loss of manganese oxide each annealed for 2 h at 100, 200, 300 and 400 °C, respectively.

This can be attributed to dehydration of structural water. As the temperature is increased to 200 °C, the rate of weight loss decreases slightly and an associated exothermic peak is observed. This is caused by decomposition of organic matter from the deposited solution. The almost constancy of weight in the intermediate range 220–450 °C may be due to a balance between the loss of residual water and some oxygen and a slight oxidation of the oxide, as reported in the literature [8]. A stepped weight loss along with a very broad exothermic peak, attributed to oxygen release [8,17,18], is clearly discernible around 500 °C. Samples used for subsequent studies are annealed at a given temperature for 2 h. The circles in Fig. 1 show the weight change of these oxides annealed at 100–400 °C. The weight of the 100 °C-annealed oxide deviates negatively from the TGA curve. The results indicate that the removal of both structural water and organic species within the deposited manganese oxide is accomplished after 100 °C heat treatment for 2 h. Since more energy can be adsorbed during prolonged heating, the decomposition of organic matter at a lower temperature (100 °C) is explained. Moreover, the weights of the 200–400 °C-annealed oxides coincide well with the TGA data and are slight heavier than that for the oxide annealed at 100 °C. A further oxidation, of the oxide caused by annealing is recognized, by the resulting gain in weight.

The chemical compositions of the manganese oxide electrodes annealed at various temperatures for 2 h are examined by EDS. Table 1 shows the Mn and O signal ratio of the spectra obtained. It is found that the oxygen content of the oxide is decreased significantly at 100 and 500 °C. This supports the suggestion of structural water and oxygen removal as discussed above in TG and DT analyses.

3.2. Crystal structure of oxide electrodes

X-ray diffraction patterns of manganese oxide electrodes annealed at various temperatures are presented in Fig. 2. The patterns of the samples annealed up to 400 °C are identical to that of the as-deposited oxide electrode. Beside the strong diffraction peaks associated with the graphite substrate, each pattern has a broad peak with very low intensity at about 37°. This weak peak, due to the contribution of manganese oxide [16], indicates that the oxides have poor crystallinity. When the treated temperature exceeds 500 °C, however, the formation of crystalline Mn_2O_3 occurs. The crystallization reaction coincides with a sharp weight loss, caused by oxygen removal, of the deposited manganese

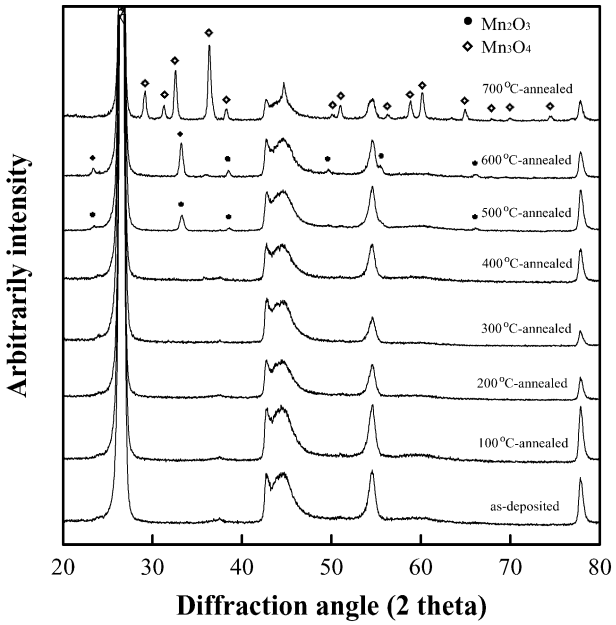

Fig. 2. X-ray diffraction patterns of manganese oxide electrodes annealed at various temperatures.

oxide, as mentioned in the previous section. Moreover, the oxide completely converts to Mn_3O_4, as demonstrated in the figure, as the temperature is raised to 700 °C. The transformation of Mn_2O_3 to Mn_3O_4 can be described by the following deduction reaction:

$$3Mn_2O_3 \rightarrow 2Mn_3O_4 + \tfrac{1}{2}O_2 \quad (1)$$

accompanied by the removal of oxygen.

3.3. Surface morphology and chemical composition of various manganese oxides

The morphology of the as-deposited manganese oxide electrode is shown in Fig. 3. At a low magnification, as illustrated in Fig. 3a, cracks and granular oxide are seen on the electrode surface. The cracks are probably caused by shrinkage stress during drying. The detail features of the manganese oxide are shown in Fig. 3b. It is found that the electrode consists of fibrous oxide with a nano-size diameter.

Surface morphologies, examined by SEM, of deposited manganese oxide annealed at various temperatures are shown in Fig. 4. The features of the fiber-like manganese oxides are still observable at 100 and 200 °C annealing, see Fig. 4a and b. The result indicates that the release of water and organic species of as-deposited manganese oxide (as

Table 1
Mn and O signal ratio of manganese oxides annealed at various temperatures from EDS analyses

Specimen	As-deposited	100 °C-annealed	300 °C-annealed	500 °C-annealed	700 °C-annealed
Mn signal ratio (%)	75.8	78.3	78.5	82.1	83.1
O signal ratio (%)	24.2	21.7	21.5	17.9	16.9

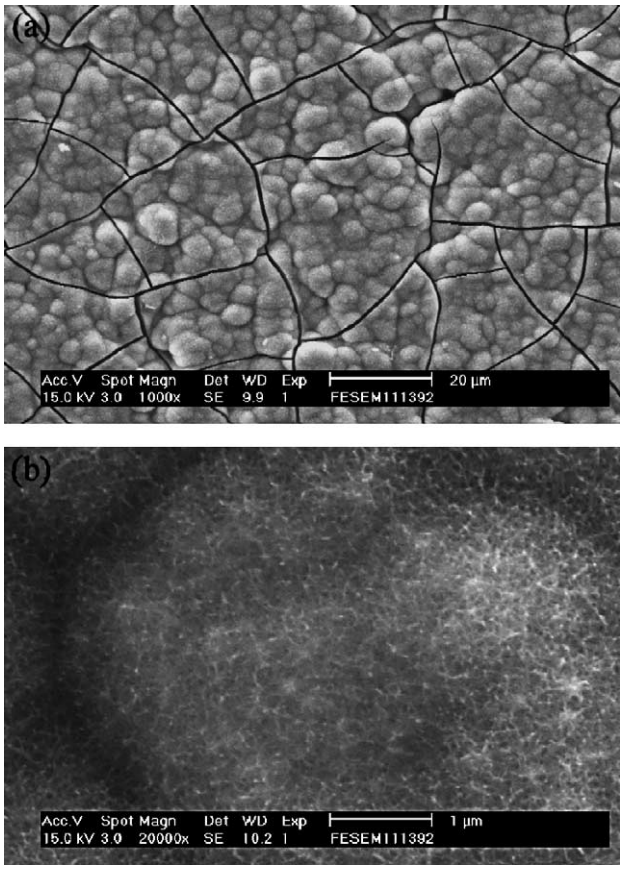

Fig. 3. SEM micrographs of as-deposited manganese oxide with different magnifications: (a) l000× and (b) 20,000×.

confirmed by TG/DT analyses) do not cause a significant change in morphology. By contrast, manganese oxides annealed at 300 and 400 °C exhibit a different appearance, see Fig. 4c and d. The fibrous oxide tends to tangle with each other. A micrograph of the deposited oxide annealed at 500 °C is presented in Fig. 4e. It is composed of many fine spherical particles. The significant change in morphology at 500 °C is considered to be caused by crystallization of the amorphous manganese oxide, since the corresponding formation of crystalline Mn_2O_3 has been determined by GAXRD analysis. As the annealing temperature is raised to 600 °C, the oxide morphology becomes rod-like (as shown in Fig. 4f). The morphology of the oxide after 700 °C heat treatment is presented in Fig. 4g. Oxide, 'islands', corresponding to the phase transformation to Mn_3O_4 (from GAXRD), can be observed.

3.4. Chemical state of various manganese oxides

A typical XPS spectra for the Mn $2p_{3/2}$ orbit of deposited manganese oxide annealed at various temperatures are given in Fig. 5. The spectra of the as-deposited, 100 °C-annealed and 300 °C-annealed oxides are similar and have peaks with a binding energy of 642.4 eV. It has been reported in [19,20] that the binding energies of the Mn $2p_{3/2}$ electron for Mn^{3+} and Mn^{4+} are 641.6 and 642.6 eV, respectively. The analytic results shown in Fig. 5 indicate that these oxides are composed of both trivalent and tetravalent manganese oxides. When the annealing temperature is increased to 500 °C, the binding energy is shifted to 641.8 eV (as revealed in the figure). Significant reduction of the oxide is evident and nearly trivalent manganese can be obtained. The existence of Mn_2O_3 at 500 °C, identified by XPS, have been previously confirmed by GAXRD.

The variation of manganese valent state with annealing temperature can be identified more specifically by investigating the multiplet splitting width of Mn 3s peaks [21,22]. The exchange interaction between the core level electron (3s) and the unpaired electrons in the valence band level (3d) results in the peak separation of the Mn 3s spectrum upon photoelectron ejection [23,24]. Accordingly, the lower valence of manganese gives rise to a wider splitting of the 3s peaks. XPS spectra for the Mn 3s orbit of the deposited manganese oxide annealed at various temperatures are shown in Fig. 6. The peak separation (ΔE) of Mn 3s spectra is clearly found to vary with heat-treatment temperature. The peak locations of Gauss-fitting results are listed in Table 2. The multiplet splittings of Mn 3s for MnO, Mn_3O_4, Mn_2O_3 and MnO_2 have been reported by Chigane and Ishikawa [21], were also shown in this Table. The peak separation, 5.24 eV, of the as-deposited manganese oxide further demonstrates that trivalent and tetravalent Mn ions co-exist within the oxide. An apparent decrease of ΔE (5.02 eV) is found when the as-deposited oxide is heated at 100 °C. This implies that the oxidation state of manganese definitely increases after 100 °C heat treatment. At 300 °C, the slight decrease of ΔE (4.98 eV) indicates a small increase in the average oxidation state. When the temperature is raised to 500 °C, a sudden increase in peak separation (5.44 eV) is observed, indicating the change of high valence manganese to form Mn_2O_3 with trivalent Mn ions.

The O 1s spectra of deposited manganese oxides annealed at various temperatures were further analyzed; the results are presented in Fig. 7. The spectra obtained can be deconvoluted into three constituents that correspond to different oxygen-containing species such as Mn–O–Mn at 529.3–530.3 eV, Mn–O–H at 530.5–531.5 eV and H–O–H

Table 2
XPS Mn 3s analytical results for manganese oxides annealed at various temperatures

Specimen	Eb1 (eV)	Eb2 (eV)	ΔE (eV)	Species [21]
As-deposited	83.95	89.19	5.24	
100 °C-annealed	83.97	88.99	5.02	
300 °C-annealed	84.01	88.99	4.98	
500 °C-annealed	83.56	89.00	5.44	
			5.79	MnO
			5.50	Mn_3O_4
			5.41	Mn_2O_3
			4.78	MnO_2

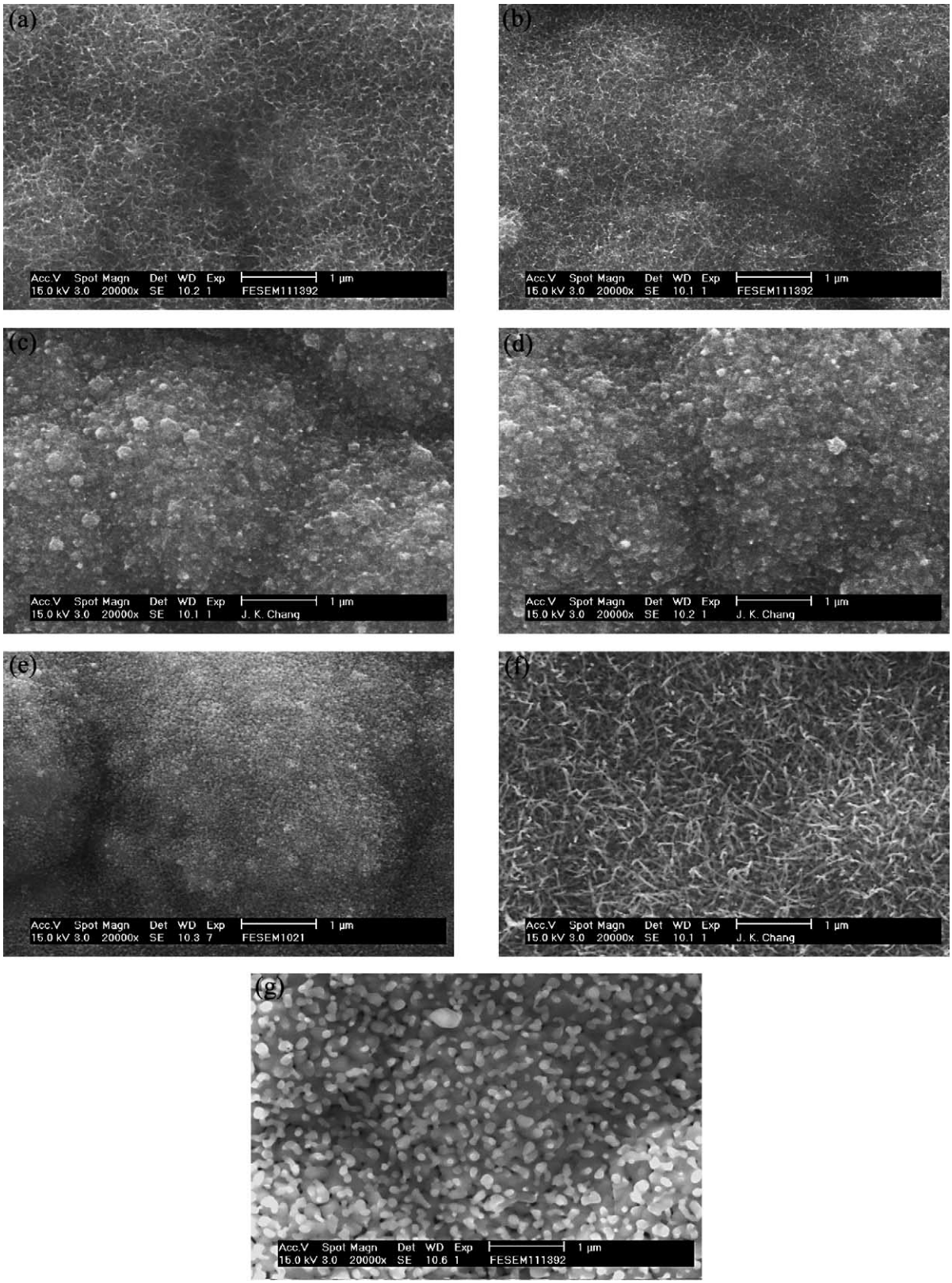

Fig. 4. SEM micrographs of manganese oxides annealed at (a) 100 °C, (b) 200 °C, (c) 300 °C, (d) 400 °C,. (e) 500 °C, (f) 600 °C and (g) 700 °C.

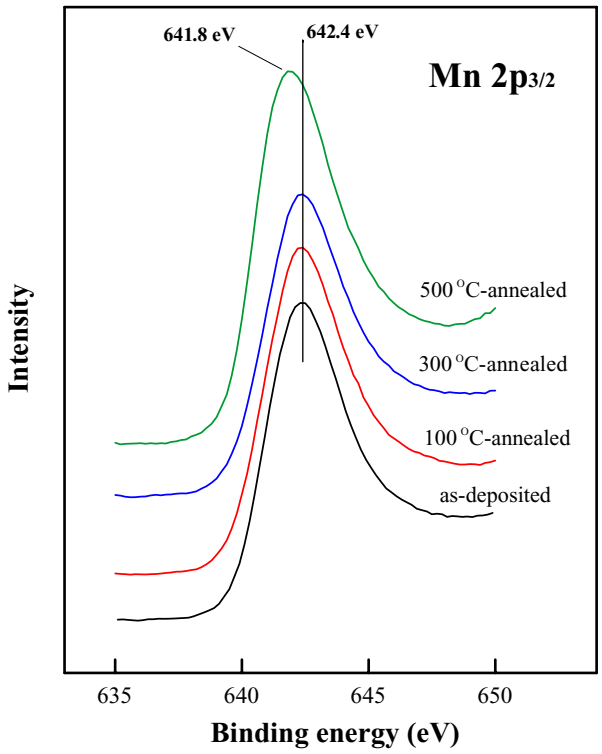

Fig. 5. XPS spectra of Mn $2p_{3/2}$ orbit for manganese oxide annealed at various temperatures.

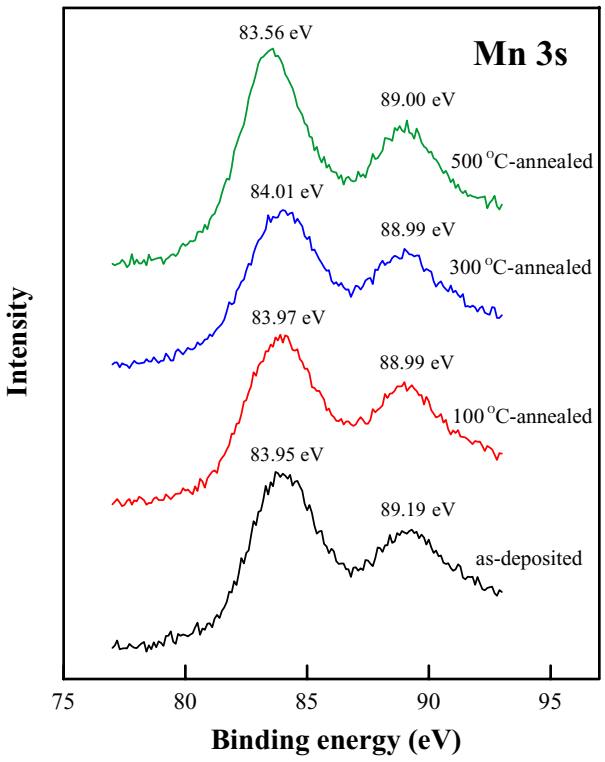

Fig. 6. XPS spectra of Mn 3s orbit for manganese oxide annealed at various temperatures.

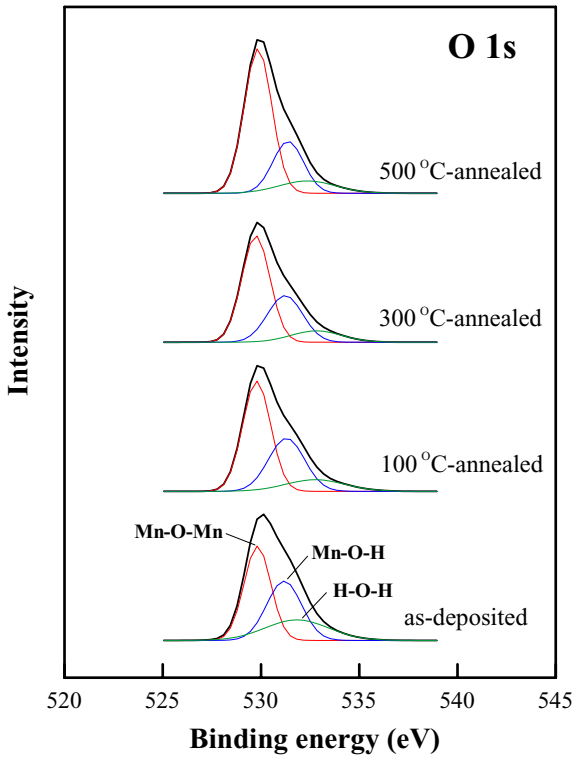

Fig. 7. XPS spectra of O 1s orbit for manganese oxide annealed at various temperatures.

at 531.8–532.8 eV [21,22]. The areas under the peaks (measured as a percentage of that under the O 1s peak) of these three species for the oxides deposited at different temperatures are summarized in Table 3. A higher percentage of area indicates a higher amount of the corresponding species in the oxide. It is found that the amounts of anhydrous oxide (i.e., Mn–O–Mn) increase while the water content decrease when the deposited manganese oxide is annealed at 100 °C. Clearly, the release of structural water and the dehydration of deposited manganese oxide can occur at this temperature. The analytical results and consistent with those previously mentioned in Section 3.1. A slight variation of the O 1s spectrum is noticeable when the heat-treatment temperature is raised from 100 to 300 °C. The amount of Mn–O–Mn species within the oxide is found to increase slightly. When the annealing temperature is increased further to 500 °C, the hydroxide component is decreased drastically and anhydrous Mn–O–Mn becomes the dominant species in the oxide.

3.5. Electrochemical characteristics

Cyclic voltammograms (CVs) of various electrodes, measured in 2 M KC1 solution at 25 °C at a potential scan rate of 5 mV s^{-1}, are shown in Fig. 8. The CV curves of the deposited oxide annealed at a low temperature (<300 °C) are close to rectangular shapes and exhibit mirror-image characteristics as shown in Fig. 8a and b. The results demonstrate

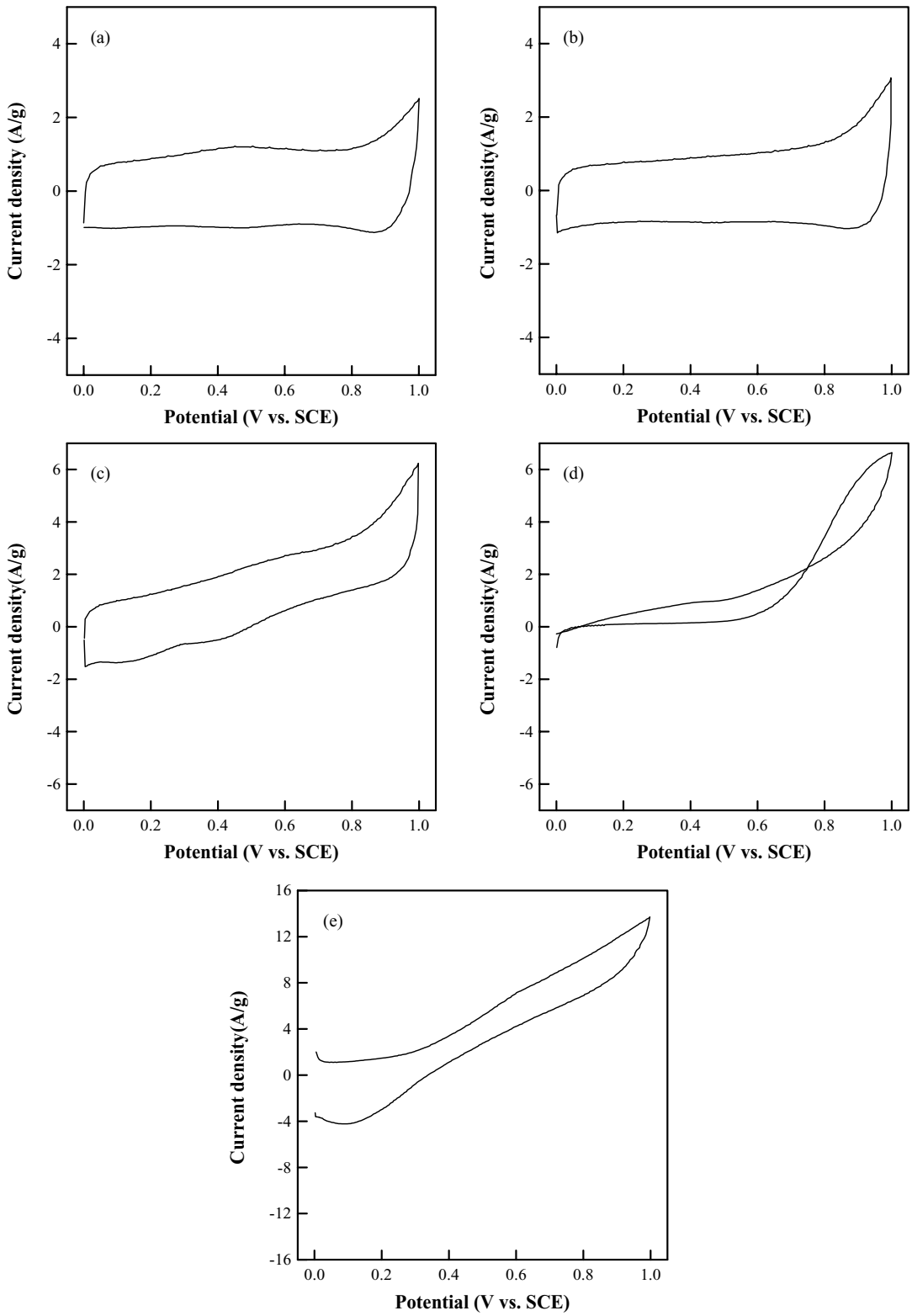

Fig. 8. Cyclic voltammograms of (a) as-prepared, (b) 100 °C, (c) 300 °C, (d) 500 °C and (e) 700 °C-annealed manganese oxide electrodes, measured in 2 M KC1 solution with a potential scan rate of 5 mV s^{-1}.

Table 3
XPS O 1s analytical results for manganese oxides annealed at various temperatures

As-deposited		100 °C -annealed		300 °C -annealed		500 °C -annealed	
Species	Peak area (%)	Species	Peak area (%)	Species	Peak area (%)	Species	Peak area (%)
Mn–O–Mn	42.8	Mn–O–Mn	54.5	Mn–O–Mn	57.4	Mn–O–Mn	63.7
Mn–O–H	35.0	Mn–O–H	33.1	Mn–O–H	31.5	Mn–O–H	25.3
H–O–H	22.2	H–O–H	12.2	H–O–H	11.1	H–O–H	11.0

the excellent reversibility and ideal pseudo-capacitive behaviour of the electrodes. The CV curve of the manganese oxide electrode annealed at 300 °C has a distorted rectangular shape (Fig. 8c). The current does not remain constant but clearly varies with the electrode potential. Moreover, the asymmetric plot, with a large enclosed anodic portion and a small cathodic one, illustrates the irreversible behaviours of the oxide electrode. Re-construction of oxide morphology, as observed by SEM in Fig. 4, may cause the physical and/or chemical properties to change and there by cause degradation of the pseudo-capacitive performance for the 300 °C-annealed manganese oxide electrode. The CV curves shown in Fig. 8d and e reveal quite different electrochemical behaviour of the manganese oxide electrodes annealed at 500 and 700 °C, respectively. At these two different heat-treatment temperatures, the formation of crystalline Mn_2O_3 and Mn_3O_4, respectively, are favoured as confirmed by GAXRD analyses. Since the crystal lattice rather than the amorphous structure is rigid and difficult to expand (or contract), retardation of the protonation (or de-protonation) reaction of the oxide electrodes is expected. The fast, continuous and reversible faradaic reaction is thus hindered, and consequently causes the loss of pseudo-capacitive properties, as demonstrated in Fig. 8d and e.

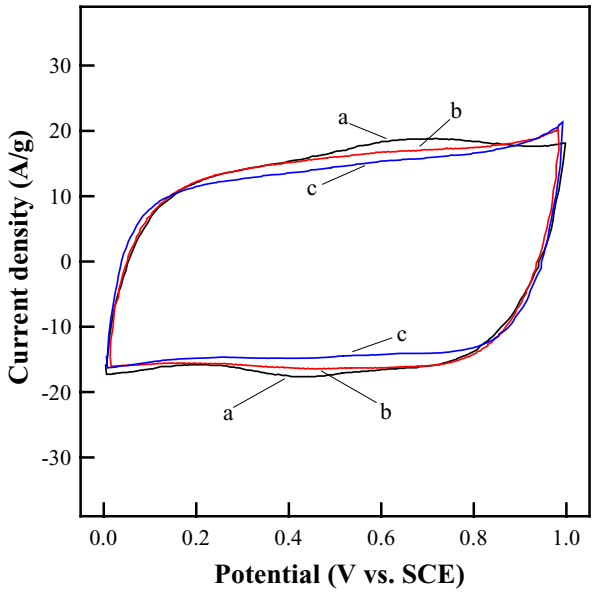

Fig. 9. Cyclic voltammograms of: (a) as-deposited; (b) 100 °C-annealed and (c) 200 °C-annealed manganese oxide electrodes in 2 M KCl solution at a potential scan rate of 150 mV s^{-1}.

The electrochemical properties of deposited manganese oxide electrodes annealed at low temperatures were further explored. The CV curves, measured at a rather high potential sweep rate of 100 mV s^{-1}, for electrodes prepared from the as-deposited manganese oxide and those annealed at 100 and 200 °C are presented in Fig. 9. The shapes of these curves are similar. Even at such a high potential sweep rate, almost ideal pseudo-capacitive behavior is observed for these three different electrodes. Moreover, the satisfactory kinetic reactivity makes them promising electrodes for use in supercapacitors. As can be seen in Fig. 9, the enclosed areas of the CV curves are different, The specific voltammetric charge of the electrodes (based on the weight of manganese oxide and integrated from positive to negative sweeps) decreases with increase in the annealing temperature. The specific capacitance (C) of the manganese oxide can be estimated as:

$$C = \frac{\text{specific voltammetric charge}}{\text{potential range}}$$

The specific capacitances of the as-deposited, 100 °C-annealed and 200 °C-annealed oxides, measured at a CV scan rate of 100 mV s^{-1}, are 149, 144 and 135 F g^{-1}, respectively. The effect of heat treatment on the specific capacitance of the manganese oxide was examined at various CV scan rates; the results are presented in Fig. 10. The monotonous decline

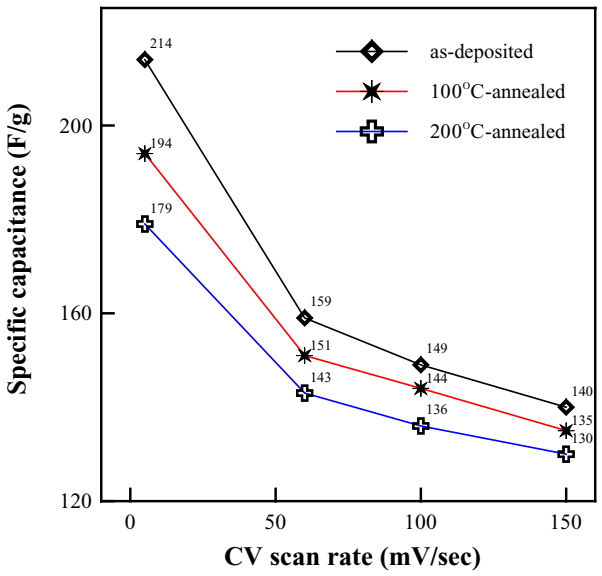

Fig. 10. Effect of heat treatment and CV scan rate on specific capacitance of manganese oxide electrodes.

of specific capacitance with increasing annealing temperature (to 200 °C) can be clearly seen. It has been reported that the presence of structural water promotes the ionic diffusivity but increases the electronic resistivity of the oxide [6,25], and causes a modification of its electrochemical performance [14,18]. The results obtained from XPS and CV analyses in this investigation support these assertions. More specifically, the release of structural water (caused by heating) will lead to a decrease in specific capacitance of the manganese oxide. Furthermore, annealing at 100 and 200 °C causes the manganese oxide to transform to a high oxidation state. As found in our previous study [16], the higher oxidation state of oxide could give a lower specific capacitance of the manganese oxide electrode. The lower specific capacitances for both annealed electrodes, as compared with that of the as-deposited one, are partly associated with the increase in oxidation state.

As revealed in Fig. 10, the specific capacitance gradually decreases as the potential scan rate is increased from 5 to 150 mV s^{-1} for all the manganese oxide electrodes. For instance, the specific capacitance of the as-deposited manganese oxide is as high as 214 F g^{-1} at a sweep rate of 5 mV s^{-1} but decreases to 140 F g^{-1} as the sweep rate is raised to 150 mV s^{-1}. The specific capacitances, at a tile CV scan rate of 5 mV s^{-1} (C_5^0) and 150 mV s^{-1} (C_{150}^0), of various manganese oxide electrodes are listed in Table 4.

The electrochemical stability of the manganese oxide was evaluated by repeating the CV test for 300 cycles. The variation of specific capacitance (at a CV scan rate of 5 mV s^{-1}) with cycle number for the electrodes annealed at different temperature is presented in Fig. 11. The specific capacitance of all the electrodes declines rapidly during the first 100 cycles but remains almost constant thereafter (until 300 cycles). The specific capacitances of the various electrodes after 300 CV cycles (C_5^*) are also given in Table 4. The specific capacitances, in terms of C_5^*/C_5^0 ratios, after 300 cycles for the as-deposited, 100 °C-annealed and 200 °C-annealed manganese oxide electrodes were 77.6, 90.2 and 97.2%, respectively. Clearly, the cyclic stability of the manganese oxide electrodes can be significantly improved by heat treatment.

Table 4
The specific capacitance of manganese oxides (annealed at various temperatures) under different test conditions

Specimen	C_5^0 (F g^{-1})	C_{150}^0 (F g^{-1})	C_5^* (F g^{-1})	$(C_5^*/C_5^0) \times 100$ (%)
As-deposited	214	140	166	77.6
100 °C-annealed	194	135	175	90.2
200 °C-annealed	179	130	174	97.2

Note: C_5^0, specific capacitance measured at the CV scan rate of 5 mV s^{-1}; C_{150}^0, specific capacitance measured at the CV scan rate of 150 mV s^{-1}; C_5^*, specific capacitance measured after 300 CV cycles at a scan rate of 5 mV s^{-1}.

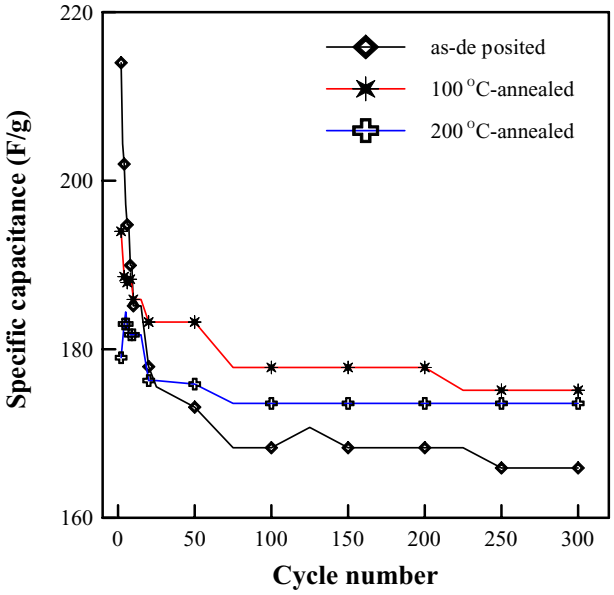

Fig. 11. Variation of specific capacitance with CV cycle number of manganese oxide electrodes annealed at various temperatures.

4. Conclusions

Manganese oxide, with an amorphous structure and a fibrous feature, is found to consist of a mixture of trivalent and tetravalent manganese. After annealing at 100 °C for 2 h, the structural water and residual organic matter of the as-deposited manganese oxide is removed. Moreover, the average oxidation state of the oxide is increased. As the temperature is raised to 300 °C, the fibrous oxide, still with an amorphous structure, tends to tangle. At 500 °C, a portion of oxygen within the oxide is released and crystalline Mn_2O_3 is formed. Further increase of the annealing temperature to 700 °C causes the formation of Mn_3O_4. Cyclic voltammetry reveals that the oxide electrodes annealed at temperatures below 200 °C exhibit excellent pseudo-capacitive properties. Although the specific capacitance decreases, the cyclic stability of the deposited manganese oxide is significantly improved with increasing annealing treatment (to 200 °C). When the oxide is annealed at 300 °C, a degradation of capacitive performance is clearly discernible, due to re-construction of the oxide morphology. The loss of pseudo-capacitive of the oxide annealed above 500 °C is caused by formation of crystalline phases.

Acknowledgements

The authors are grateful to the National Science Council of the Republic of China for financially supporting this research under Contract No. NSC 92-2216-E-006-043.

References

[1] B.E. Conway, Electrochemical Supercapacitors, Kluwer Academic/Plenum Publishers, New York, 1999.

[2] B.E. Conway, J. Electrochem. Soc. 138 (1991) 1539.
[3] S. Sarangapani, B.V. Tilak, C.P. Chen, J. Electrochem. Soc. 143 (1996) 3791.
[4] G.L. Bullard, H.B. Sierra-Alcazar, H.L. Lee, J.L. Morris, IEEE Trans. Magnet. 25 (1989) 102.
[5] J.P. Zheng, T.R. Jow, J. Electrochem. Soc. 142 (1995) L6.
[6] J.P. Zheng, P.J. Cygan, T.R. Jow, J. Electrochem. Soc. 142 (1995) 2699.
[7] Y. Takasu, T. Nakamura, H. Ohkawauchi, Y. Murakami, J. Electrochem. Soc. 144 (1997) 2601.
[8] C. Tsang, J. Kim, A. Manthiram, J. Solid State Chem. 137 (1998) 28.
[9] Y.U. Jeong, A. Manthiram, J. Electrochem. Soc. 149 (2002) A1419.
[10] H.Y. Lee, V. Manivannan, J.B. Goodenough, Comptes Rendus Chimie 2 (1999) 565.
[11] H.Y. Lee, J.B. Goodenough, J. Solid State Chem. 144 (1999) 220.
[12] S.C. Pang, M.A. Anderson, T.W. Chapman, J. Electrochem. Soc. 147 (2000) 444.
[13] S.C. Pang, M.A. Anderson, J. Mater. Res. 15 (2000) 2096.
[14] S.F. Chin, S.C. Pang, M.A. Anderson, J. Electrochem. Soc. 149 (2002) A379.
[15] C.C. Hu, T.W. Tsou, Electrochem. Commun. 4 (2002) 105.
[16] J.K. Chang, W.T. Tsai, J. Electrochem. Soc. 150 (2003) A1333.
[17] H. Ikeda, US Patent 4,133,856.
[18] H. Kim, B.N. Popov, J. Electrochem. Soc. 150 (2003) D56.
[19] B.R. Strohmeier, D.M. Hercules, J. Phys. Chem. 88 (1984) 4922.
[20] B.N. Ivanov-Emin, N.A. Nevskaya, B.E. Zaitsev, T.M. Ivanova, Russ. J. Inorg. Chem. 27 (1982) 1755.
[21] M. Chigane, M. Ishikawa, J. Electrochem. Soc. 147 (2000) 2246.
[22] M. Chigane, M. Ishikawa, M. Izaki, J. Electrochem. Soc. 148 (2001) D96.
[23] J.C. Carver, G.K. Schweitzer, T.A. Carlson, J. Chem. Phys. 57 (1972) 973.
[24] M. Oku, K. Hirokawa, S. Ikeda, J. Electron Spectrosc. Relat. Phenom. 7 (1975) 465.
[25] S.B. Kanungo, K.M. Parida, B.R. Sant, Electrochim. Acta 26 (1981) 1147.